JOURNAL OF SOLID STATE CHEMISTRY 25, 263–271 (1978)

Influence of Crystallite Size on the Oxidation Kinetics of Magnetite

B. GILLOT,*[1] A. ROUSSET,† AND G. DUPRE‡

*Laboratoire de Recherches sur la Réactivité des Solides associé au C.N.R.S. Faculté des Sciences Mirande 21000 Dijon, France,
†Laboratoire de Chimie des Matériaux Inorganiques, Université Paul Sabatier, Toulouse III, 118 route de Narbonne, 31000 Toulouse, France, and
‡Laboratoire de Chimie Minérale, Université Claude Bernard, Lyon 1–43 Boulevard du 11 Novembre 1918, 69621, Villeurbanne, France

Received May 14, 1977

The oxidation of magnetite yields the lacunar phase γ-Fe_2O_3, for sizes less than 5000 Å and the rhombohedral phase, α-Fe_2O_3, for sizes above 10 000 Å. For intermediate sizes, oxidation kinetics and X-ray analysis have confirmed that the γ-Fe_2O_3 phase forms at the beginning of the reaction, followed by phase α-Fe_2O_3 forming from γ-Fe_2O_3 and then directly from the still-unoxidized magnetite. Influence of size could be accounted for in terms of structure and stresses at the crystal lattice level.

Introduction

Feitknecht *et al.* (*1–4*) had already shown that, depending on magnetite crystallite size, either phase γ-Fe_2O_3 with similar, cubic but lacunar structure could be obtained according to:

$$Fe_3O_4 \rightarrow Fe_{3-x}O_4 \rightarrow \gamma\text{-}Fe_2O_3,$$

or the rhombohedral phase α-Fe_2O_3 according to:

$$Fe_3O_4 \rightarrow Fe_{3-x}O_4 \rightarrow \alpha\text{-}Fe_2O_3 +$$
$$Fe_3O_4 \xrightarrow{\text{temperature rise}} \alpha\text{-}Fe_2O_3,$$

the critical size being close to 3000 Å.

Alternatively, Colombo (*5*, *6*) maintained that size was not the governing factor for obtaining γ-Fe_2O_3 and that nuclei from the α-Fe_2O_3 phase or stacking faults initially present in magnetite were required to obtain the α-Fe_2O_3 phase. In addition, he maintained that the γ-Fe_2O_3 phase could only be obtained from disordered magnetite.

But Colombo used samples of natural magnetite containing some impurities, which could stabilize the γ-Fe_2O_3 phase whereas the synthetic samples used by Feitknecht were always partially oxidized, since for sizes about 2000 Å, the amount of Fe^{2+} ions never exceeded 26% of total iron compared to the theoretical value, 33.33%. This may have given rise to the disagreement between both authors.

Influence of crystallite size on reaction activation energy could be shown on investigating the kinetics of the oxidation of aluminum-substituted magnetite, $(Fe^{2+}Fe^{3+}_{2-x}Al^{3+}_x)O_4^{2-}$, to the lacunar phase $\gamma(Fe^{3+}_{1-y}Al^{3+}_y)_2O_3^{2-}$ ($0 < x < 2$ and $x = 3y$) (*7*). So, during the oxidation of pure magnetite ($x = 0$), this energy rises from 23.70 to 27.90 kcal mole^{-1} when size increases

[1] All correspondence should be addressed to B. Gillot, Laboratoire de Recherches sur la Réactivité des Solides associé au C.N.R.S., Faculté des Sciences Mirande 21000 Dijon, France.

0022-4596/78/0253-0263$02.00/0

TABLE I

SAMPLE CHARACTERISTICS

Sample	Specific area in m^2/g	Size (Å)	Oxidation range (°C)	TDA peak	
				Oxidation	$\gamma \rightarrow \alpha$
Fe_3O_4(MP)	110	90	80–170	120	490
Fe_3O_4(A)	16.3	600	150–255	140	470
Fe_3O_4(B)	12.9	900	175–260	170	460
Fe_3O_4(C)	8	1400	190–280	230	380
Fe_3O_4(D)	1.17	6000	240–320	290	460
Fe_3O_4(E)	0.80	9000	280–380	300	480
Fe_3O_4(F)	0.50	15 000	300–600	350	
Fe_3O_4(F)1	0.65	11 000			
Fe_3O_4(F)2	0.80	9000			
Fe_3O_4(F)3	1.50	5000			

from 600 to 1400 Å; for ferrialuminate ($x = 0.27$) it rises from 22.80 to 32.85 kcal $mole^{-1}$ when size increases from 200 to 3400 Å. For the latter size, the oxidized product contains tiny amounts (3 to 4%) of the rhombohedral α-phase (*8*).

The present paper deals with the oxidation kinetics and X-ray analysis of magnetite

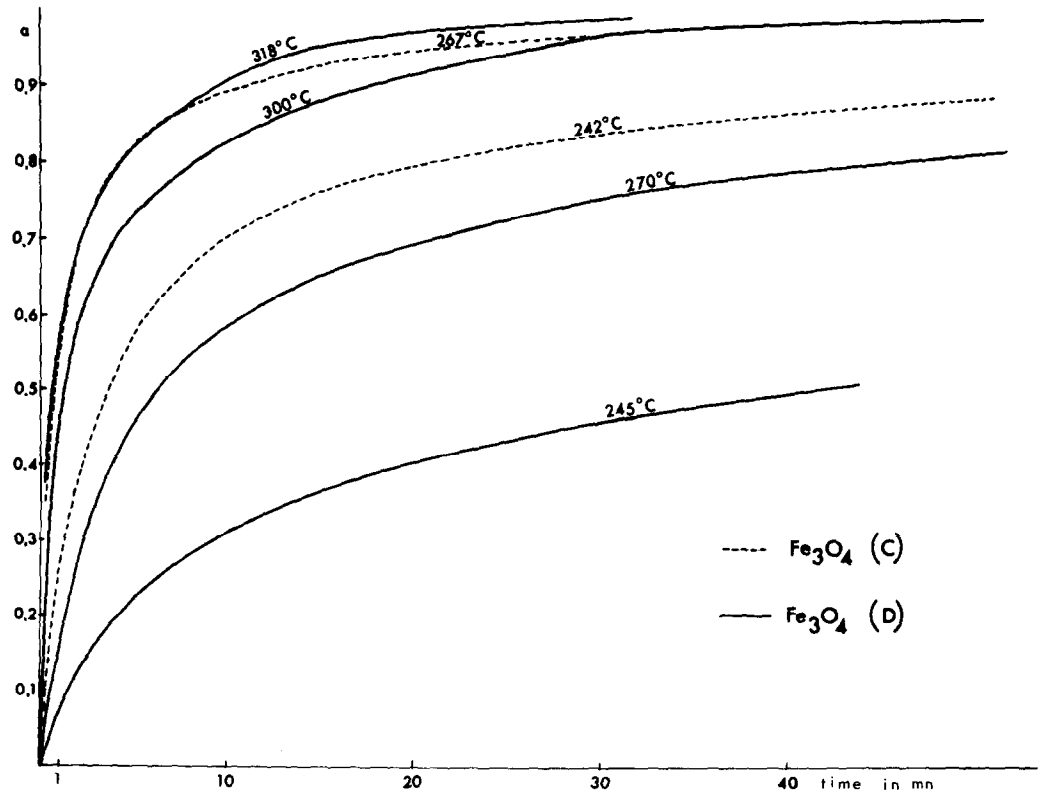

FIG. 1. $\alpha = f(t)$ curves of Fe_3O_4(D) oxidation.

samples of large size variation (100–15,000 Å) to supplement previous results concerning oxidation to the γ-Fe_2O_3 phase (*7*) and to understand better the formation process of the α-Fe_2O_3 phase in the presence of γ-Fe_2O_3.

Samples

Preparation conditions of samples (A), (B), (C), and (D) (Table I) have already been fully stated (*9*, *10*). It may be recalled that an iron sesquioxide of given granulometry is submitted to an oxido-reducing treatment. This α-Fe_2O_3 sesquioxide is obtained by decomposition of $(NH_4)_3\,[Fe(C_2O_4)_3]\cdot 3\,H_2O$ in air. The salt decomposition temperatures, those of reduction, and the water vapor content in hydrogen govern the average crystallite size. For samples (E) and (F) those treatments were followed by annealing under vacuum at 800 and 1000°C, respectively. Sample (MP) consisting of small crystallites of 100 Å was obtained in the wet way by heat treatment of adequate amounts of a solution of ferrous and ferric salts in a solution of ammonia.

The characteristics are listed in Table I. Iron titration shows that the Fe^{2+} content versus total iron is above 32% for those samples whose average crystallite sizes are over 600 Å (theoretical value 33.33%) whereas the adsorbed water content becomes negligible. The Fe^{2+} percentage is 31% in sample (A) whereas it is only 12% in sample (MP) whose stability is low with respect to oxygen from room temperature. The latter sample contains an adsorbed water content as high as 8%.

The techniques used to characterize these samples, namely, X-ray analysis, S.E.M., and D.T.A., have also been already reported (*9*, *10*).

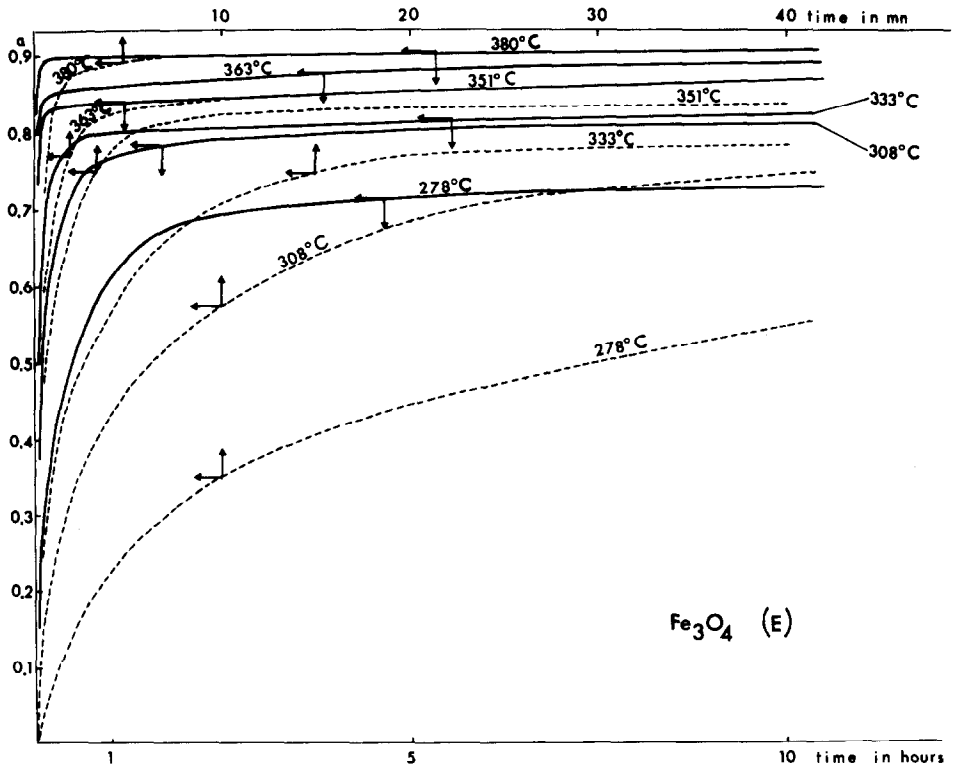

FIG. 2. $\alpha = f(t)$ curves of Fe_3O_4(E) oxidation.

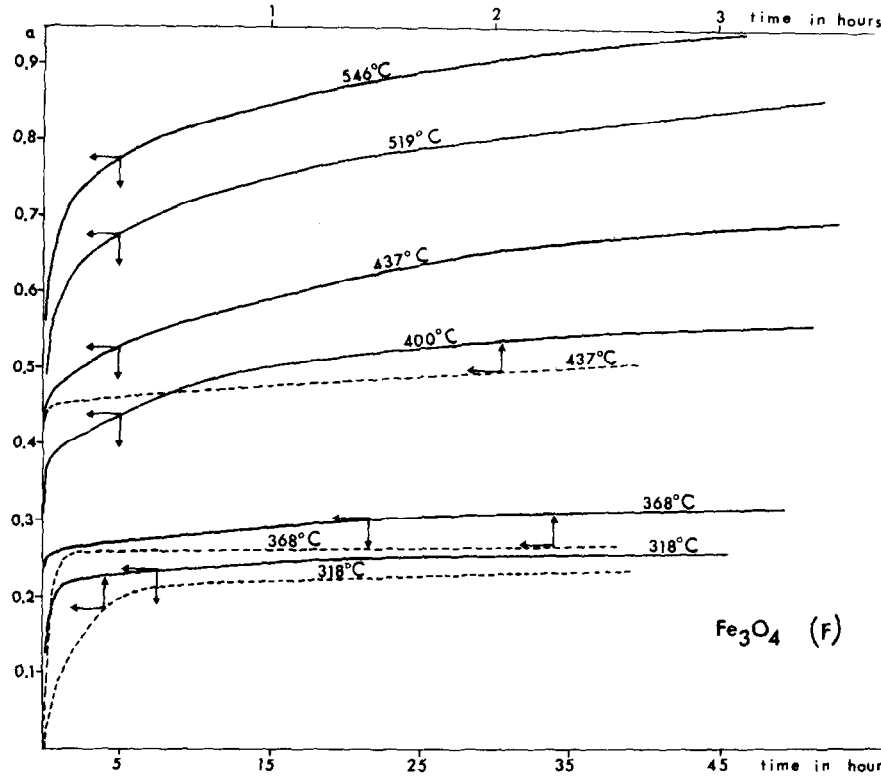

FIG. 3. $\alpha = f(t)$ curves of Fe_3O_4(F) oxidation.

Results

1. *Kinetic Study*

The technique used to investigate total or partial oxidation and the results concerning magnetites (A), (B), and (C) have also been reported (*7*, *11*). It has been especially shown that the $\alpha = f(t)$ curves (α = conversion ratio) follow the same course in time. The same holds for curves relative to the oxidation of Fe_3O_4(MP).

The kinetic curves of Fe_3O_4(D), (E), and (F) oxidation are plotted in Figs. 1, 2 and 3. Figure 1 also shows two oxidation curves of Fe_3O_4(C). The oxidation ranges are listed in Table I.

The Fe_3O_4(D) curves showed an affinity up to a conversion ratio $\alpha = 0.80$ and those of Fe_3O_4(E) up to about $\alpha = 0.45$. The Fe_3O_4(F) curves did not show any affinity, at least for reaction temperatures less than 500°C. Variation of the affinity ratio versus temperature allows the experimental activation energy to be calculated. It is 38 kcal mole^{-1} for Fe_3O_4(D) and 39.3 kcal mole^{-1} for Fe_3O_4(E),

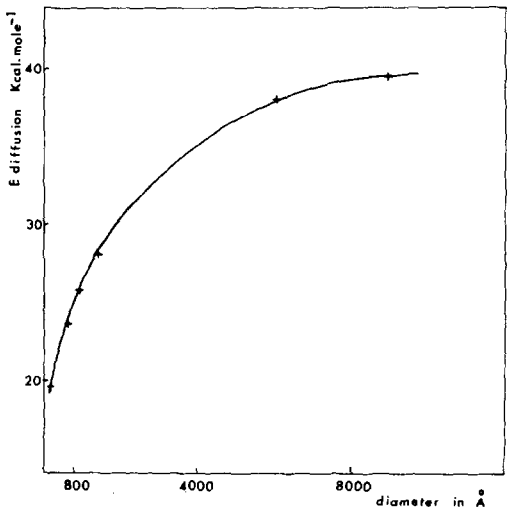

FIG. 4. Evolution of the experimental activation energy with pure magnetite crystallite size.

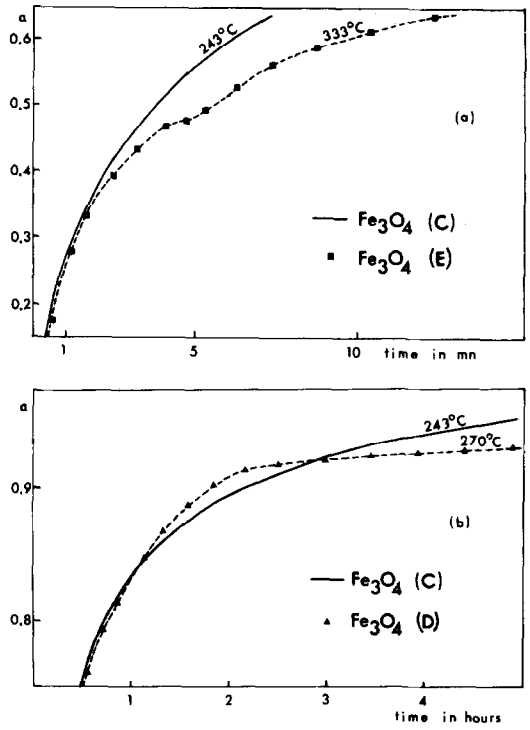

FIG. 5. Evolution of the $\alpha = f(t)$ curves of (a) Fe_3O_4(E) and (b) Fe_3O_4(D) with the curves of Fe_3O_4(C).

in agreement with what had already been observed (*7*) that energy rises with crystallite size (Fig. 4).

Beyond $\alpha = 0.80$ for Fe_3O_4(D) and $\alpha = 0.45$ for Fe_3O_4(E), the curves have no longer any affinity and, compared to Fe_3O_4(C), a different behavior is observed, which for Fe_3O_4(D) results in a more rapid reaction followed by a slowing down (Fig. 5b), and for Fe_3O_4(E) in a pseudostage also followed by a slowing down (Fig. 5a). For Fe_3O_4(F) acceleration occurs from the beginning of the reaction (Fig. 3) followed by a slowing down, then a blocking, such that the higher the temperature the greater the extent of reaction, e.g., at 318°C, the conversion ratio cannot be over $\alpha = 0.25$; the temperature has to be raised above 500°C to obtain total oxidation, which in this case takes several days.

In the case of Fe_3O_4(F), for temperatures above 500°C, however, as isotherm network could be plotted; for $\alpha > 0.5$, the $\alpha = f(t)$ curves are superimposable in an affinity versus time. They are transformed into straight lines using $\frac{2}{3}\alpha + (1 - \alpha)^{2/3} - 1 = kt$ obtained in spherical symmetry by solving the elementary-step equations in which only the diffusion step is not in quasi-equilibrium (*12*). In addition, the calculation uses the expansion coefficient Δ as being 1, which may be easily justified, as the Fe_3O_4 and Fe_2O_3 specific weights are close to each other. Influence of temperature on reaction rate results in an apparent activation energy of 51 ± 2 kcal mole^{-1} related to the diffusion process in a biphase medium (*13*). This value is close to that obtained by Channing *et al.* for α-Fe_2O_3 growth from Fe_3P_4 (*14*).

2. *X-Ray Analysis*

Oxidation was jointly followed by X-ray analysis for various conversion ratios. The results are listed in Table II. For Fe_3O_4(D), a lacunar spinel phase is first obtained whose composition lies between Fe_3O_4 and γ-Fe_2O_3

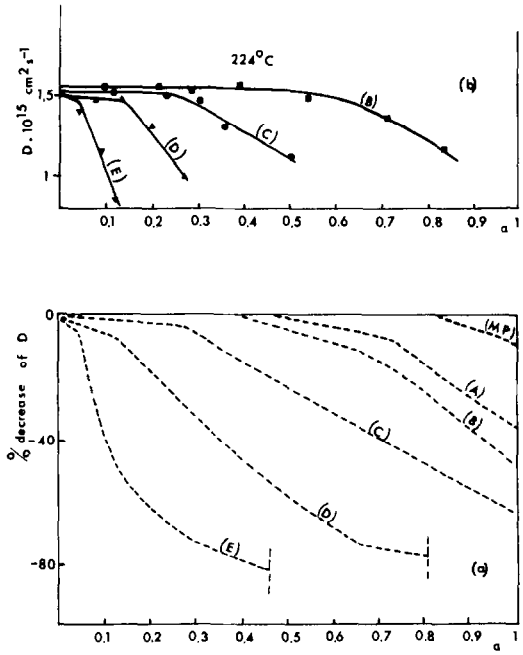

FIG. 6. Change in the diffusion coefficient D *vs* α for various magnetite sizes (a) % of decrease of D, (b) ecrease of D for a similar temperature of 224°C.

TABLE II

PHASES OBTAINED BY X-RAY ANALYSIS

Conversion ratio (α)	Oxidation temperature (°C)	Phase obtained
		Fe_3O_4(D)
0.30	300	Lacunar spinel without superstructure rays
0.41	300	Lacunar spinel without superstructure rays
0.71	300	Lacunar spinel with superstructure rays
0.80	300	Lacunar spinel with superstructure rays + α-Fe_2O_3 (traces)
0.91	300	Lacunar spinel with superstructure rays + α-Fe_2O_3
0.96	300	α-Fe_2O_3 + spinel phase (traces)
0.93	270	α-Fe_2O_3 + spinel phase
		Fe_3O_4(E)
0.40	280	Lacunar spinel with superstructure rays
0.55	320	Lacunar spinel with superstructure rays + α-Fe_2O_3 (traces)
0.63	320	Lacunar spinel + α-Fe_2O_3 + spinel phase
0.76	320	α-Fe_2O_3 + spinel phase
0.82	318	α-Fe_2O_3 + spinel phase
0.96	380	α-Fe_2O_3 + spinel phase
		Fe_3O_4(F)
0.24	312	α-Fe_2O_3 + spinel phase
0.42	448	α-Fe_2O_3 + spinel phase
0.90	519	α-Fe_2O_3 + spinel phase
0.97	546	α-Fe_2O_3 + spinel phase (traces)
		Fe_3O_4(F) ground
0.45 (1)	312	Lacunar spinel + α-Fe_2O_3 + spinel phase
0.45 (2)	312	Lacunar spinel + α-Fe_2O_3
0.45 (3)	312	Lacunar spinel
0.78 (2)	312	Lacunar spinel + α-Fe_2O_3 (traces)
0.97 (3)	318	Lacunar spinel

and which, from a structural standpoint, may be written as: $Fe^{3+}[\square_\delta Fe^{2+}_{1-3\delta}\, Fe^{3+}_{1+2\delta}]O_4^{2-}$ (with $\delta = \frac{1}{3}$ when oxidation is complete).

It is to be noticed that this homogeneous, mixed phase with lacunar spinel structure shows superstructure rays from $\alpha = 0.50$ (Table II), which involves a vacancy-ordering on octahedral sites occurring well before $\delta = \frac{1}{3}$, corresponding to γ-Fe_2O_3. As advocated by some authors (*15*), however, the latter compound only should favor a vacancy ordering since the ratio of the vacancy number to cation number in the same type of site is $\frac{1}{2}$. As will be shown later, it is not unlikely that there is a higher vacancy concentration in a layer close to the surface, which would make possible a vacancy ordering on octahedral sites.

For Fe_3O_4(E), the α-Fe_2O_3 phase occurs at $\alpha = 0.50$, and for Fe_3O_4(F) it is obtained from the beginning of the reaction. In all cases, traces of the spinel phase along with the rhombohedral α phase are almost always obtained at the end of the reaction. The amount of spinel phase identified as magnetite, however, depends on oxidation temperature. Thus, in the case of Fe_3O_4(D) this phase is larger when oxidation occurs at 270°C than at 310°C. It has also been noticed that temperature affects the α phase occurrence during oxidation. Thus, for Fe_3O_4(E) it may occur

for a conversion ration above $\alpha = 0.50$ if the temperature is high. This is especially due to the kinetics of the transformation $\gamma \rightarrow \alpha$ (*16*), for in the latter case oxidation to the γ-phase occurs within short times, which prevent the α-phase from forming.

Discussion

As already accounted for (*7*), the profile of kinetic curves and their affinity relative to the oxidation of Fe_3O_4(A), (B), and (C) to the lacunar γ-Fe_2O_3 phase shows that the reaction is solely ruled by bulk ionic diffusion, which must be considered under variable working conditions. In addition, this has resulted in the assumption that the diffusion coefficient D used to resolve Fick's second law in spherical symmetry was not constant but declined as the reaction proceeded. This decrease, however, was crystallite-size dependent (*7*) and the plot, the percentage of D decrease versus conver-

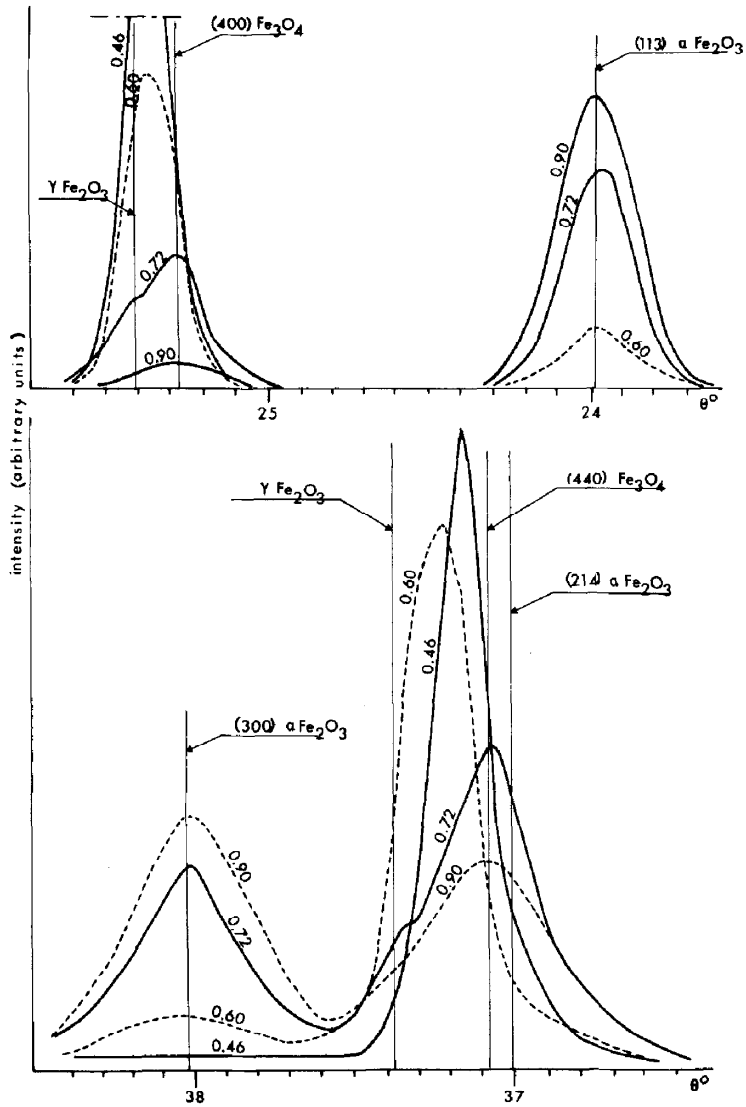

FIG. 7. Nature of the phases obtained by X-ray analysis over oxidation of Fe_3O_4(E) for various conversion ratios.

sion ratio, adequately showed this phenomenon (*8*), which was in agreement with Feitknecht's results on the oxidation of submicronic-sized magnetites (*3*).

In the present paper, a similar situation of Fe_3O_4(MP), whatever α; of Fe_3O_4(D) ($\alpha < 0.80$); and Fe_3O_4(E) ($\alpha < 0.50$) allows a similar mechanism to be considered as far as magnetite oxidizes to a homogeneous, mixed phase. Figure 6a shows the decreasing percentage of D versus α for the various crystallite sizes. These curves show that, for grains about 100 Å with a somewhat disordered lattice (X-rays are diffuse), the diffusion coefficient is practically constant. The structural disorder may then be assumed as promoting migration. For sizes between 600 and 900 Å, the bigger the crystallites, the lower the diffusion coefficient over the reaction. It is, however, found that for a similar temperature, i.e., 224°C, it remains constant whatever the size for a layer of 100 to 200 Å, which represents—for grains about 6000 Å—an extent of reaction less than $\alpha = 0.10$ (Fig. 6b). The diffusion coefficient in this layer, thus, is not affected by annealing. But above this thickness and for bigger grains, the crystal stacking is improved, which may hinder ion diffusion during the reaction. The substantial concentration change then occurs in a layer close to the surface, whereas grain-core concentration remains close to equilibrium. For Fe_3O_4(E) this results, at a conversion extent as low as $\alpha = 0.40$, in a layer rich in vacancies at the surface (almost pure γ-Fe_2O_3) whereas at the grain core the layer is far less rich in vacancies. Stresses may occur in the lattice and promote the formation of nuclei in the fresh α-rhombohedral phase owing to the difference in the lattice parameter between the thin, superficial area and the grain core. Therefore, α-Fe_2O_3 forms from the superficial γ-Fe_2O_3 and that phase whose composition nears that of magnetite is directly converted into the α-phase, which causes the profile of the kinetic curves to change beyond a given conversion ratio.

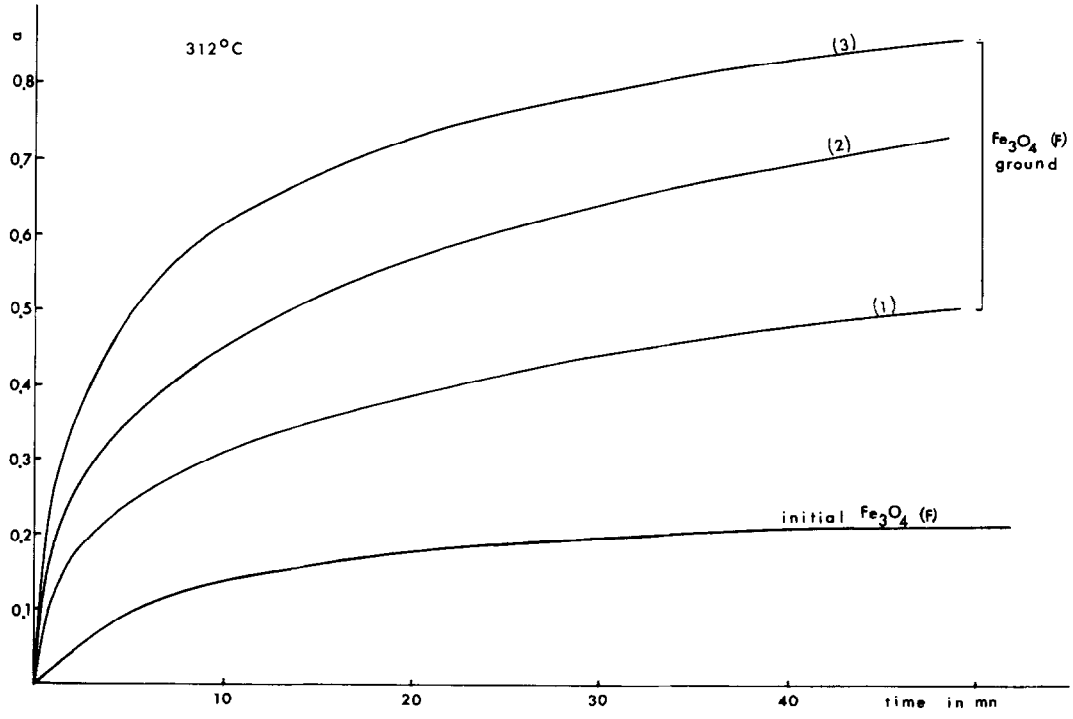

FIG. 8. Influence of grinding on the oxidation kinetics of Fe_3O_4(F).

This assumption has been confirmed by Feitknecht (*1*) and the present authors through X-ray analysis of the (440) and (400) rays of magnetite(E) during oxidation (Fig. 7). First, oxidation to a homogeneous, mixed phase was observed, causing the rays to shift and broaden as the reaction proceeded ($\alpha = 0.46$); then, from a given conversion ratio ($\alpha = 0.60$), further rays occurred due to the α-Fe_2O_3 phase. For higher conversion ratios ($\alpha = 0.72$ and $\alpha = 0.90$), the (440) and (400) rays of magnetite resumed their initial position while the α-Fe_2O_3 rays increased considerably.

A similar sample of magnetite (F) was used to show even better the role played by size in oxidation to phase γ or α; as has been seen, this magnetite oxidizes only to α-Fe_2O_3. Smaller sizes could be obtained (see Table I) by grinding the magnetite in a mortar for various lengths of time (10 min, 30 min, and 1 hr). The previous results are confirmed by oxidation kinetics (Fig. 8) and the phases obtained for $\alpha = 0.45$ (Table II). Indeed, it is observed that, whereas the smaller the crystals the higher the oxidation rate, the homogeneous, mixed phase with a spinel structure occurs first, followed by the α-Fe_2O_3 phase for the first grinding, and the homogeneous, mixed phase alone, whatever the conversion ratio, occurs for the most finely ground magnetite (third grinding). In the latter case, an isotherm set could be plotted over the temperature range 270 to 350°C and the reaction activation energy could be calculated. It is 37.8 kcal $mole^{-1}$, i.e., very close to that of Fe_3O_4(D) of similar size.

Conclusion

The present paper has shown that the size of Fe_3O_4 crystallites, indeed, is the governing factor for obtaining either the γ- or α-Fe_2O_3 phase. Temperature of annealing being the sole factor involved in the preparation of those magnetites, it should no longer be assumed, as some authors still do, that stabilizing impurities (Na or Al) initially present in Fe_3O_4, or even H_2O traces, are elements which may promote the formation of either phase. Formation of the nuclei in the fresh α-Fe_2O_3 phase is rather due to the various stresses occurring either at preparation temperature or during grinding, which, as has been pointed out, change the concentration gradient in the grain thickness and hence the diffusion coefficient.

References

1. W. Feitknecht, *Pure Appl. Chem.* **9**, 423 (1964).
2. K. Egger and W. Feitknecht, *Helv. Chim. Acta* **45**, 2042 (1962).
3. K. J. Gallagher, W. Feitknecht, and U. Mannweiler, *Nature* **217**, 1118 (1968).
4. W. Feitknecht and K. J. Gallagher, *Nature* **228**, 548 (1970).
5. U. Colombo, *Science* **147**, 1033 (1965).
6. U. Colombo, *Nature* **202**, 175 (1964).
7. B. Gillot, J. Tyranowicz, and A. Rousset, *Mater. Res. Bull.* **10**, 775 (1975).
8. J. Tyranowicz, Thèse de 3ème cycle, Dijon (1974).
9. A. Rousset, Thèse, Lyon (1969).
10. A. Rousset, J. Paris, and P. Mollard, *Ann. Chim.* **7**, 119 (1972).
11. B. Gillot, D. Delafosse, and P. Barret, *Mater. Res. Bull.* **8**, 1431 (1973).
12. P. Barret, Cinétique hétérogène, Gauthier-Villars, Paris (1973).
13. M. H. Davies, M. T. Simnard, and C. E. Birchenall, *Trans. AIME Soc. Metals* **3**, 889 (1951).
14. D. A. Channig and M. J. Graham, *Corrosion Sci.* **12**, 271 (1972).
15. J. C. Joubert, Thèse, Grenoble (1965).
16. W. Feitknecht and U. Mannweiler, *Helv. Chim. Acta* **50**, 570 (1967).